Pressure-induced decomposition of binary lanthanum intermetallic compounds

Xin Yang,[1] Hefei Li,[1] Hanyu Liu,[1] Hui Wang,[1] Yansun Yao,[2,*] and Yu Xie[1,†]

[1]*International Center for Computational Method and Software & State Key Laboratory for Superhard Materials & Key Laboratory of Physics and Technology for Advanced Batteries (Ministry of Education), College of Physics, Jilin University, Changchun 130012, China*

[2]*Department of Physics and Engineering Physics, University of Saskatchewan, 116 Science Place, Saskatoon, Saskatchewan S7N 5E2, Canada*

(Received 23 December 2019; revised manuscript received 29 March 2020; accepted 8 April 2020; published 18 May 2020)

We present a comprehensive study on structural and electronic properties of lanthanum intermetallic compounds (M_xLa_y, M = Be, Mg, Al, Ga, In, Tl, Pb, and Bi) under high pressure. By using a swarm intelligence structure search method combined with first-principles calculations, pressure-induced phase transitions of M_xLa_y were investigated, with several new structures predicted. A universal yet intriguing phenomenon was found; that is, all of these compounds will decompose into elemental solids at certain pressures, which is against the general intuition that extreme pressure always stabilizes and densifies materials. Mechanical analysis suggests that this anomalous behavior is associated to the elastic moduli and interatomic interaction in M_xLa_y, and their changes under extreme pressure. A low bulk modulus and larger atomic volume of La result in a smaller volume for the elemental mixture compared to their compound at high pressures, which leads to an energetically favorable PV work and enthalpy for the elemental mixture. Furthermore, the external pressure tends to weaken the La-M electrostatic interaction in compounds as evidenced by the reduced charge transfer between La and M, which in turn modifies the electronegativity of La and M and destabilizes the compounds. Our results shed light on the high-pressure behaviors of La-based intermetallic compounds and provide important guidance for understanding other La-like intermetallic compounds at high pressures.

DOI: 10.1103/PhysRevB.101.184113

I. INTRODUCTION

Lanthanum compounds have attracted great attention due to their various potentials industrial applications and growing applications in industry, such as usage in permanent magnets, lamp phosphors, rechargeable batteries, metallurgy, catalysts, and ceramics [1–8]. Lanthanum perovskites ($LaMO_3$) is one of the most studied lanthanum compounds [9–14]. For instance, the $LaAlO_3/SrTiO_3$ interface exhibits multiple interesting properties including superconductivity, ferromagnetism, and electric-field-controlled metal-insulator and superconductor-insulator transitions [9]. A unique feature for this interface is the coexistence of magnetism and superconductivity in the same material, which are in general mutually exclusive phenomena.

Besides lanthanum perovskites, lanthanum intermetallic compounds are also of increasing interest because of their versatile and outstanding properties [15–22]. For instance, Pt_5La was reported to be an excellent electrocatalyst for oxygen reduction reactions due to its large kinetic current density (about three times of that of Pt) [21]. Ni-La alloys, on the other hand, are promising materials for hydrogen storage. The storage capacity of Ni_5La is 1.43 wt% at room temperature. The main advantage of Ni_5La for hydrogen storage is that it can absorb and liberate hydrogen under near-ambient conditions [22]. BiLa exhibits exotic magnetotransport properties, including an extremely large and anisotropic magnetoresistance, which may find applications in magnetic valves, sensors, and memory devices [18,19]. Although considerate effort has been devoted to understanding the properties of lanthanum intermetallic compounds at ambient conditions, their properties at extreme conditions are not well studied.

As an important thermodynamic stimulus, extreme pressure can be used to modify the chemical reactivity of elements and produce materials that are not accessible at ambient conditions [23–30]. Lanthanum germanides, Ge_3La and Ge_5La, have been synthesized under high-pressure and high-temperature (HPHT) conditions and show superconductivity at 7 K [31,32]. More interestingly, LaH_{10}, a theoretically predicted high-pressure phase of lanthanum hydride, has been experimentally synthesized with measured superconducting critical temperature T_c of 250 and 260 K at 170 and 190 GPa, respectively, which are the highest T_c ever observed in all known materials [33–37]. Clearly, lanthanum intermetallic compounds tend to have technologically important properties at high pressures. Thus, it is an urgent need to explore the high-pressure properties of lanthanum intermetallic compounds.

In this work, we report a systematic study of the high-pressure behaviors of a series of intermetallic compounds between lanthanum and main group metals (M_xLa_y, M = Be, Mg, Al, Ga, In, Tl, Pb, and Bi). A common pressure-induced decomposition into individual elements is identified for M_xLa_y. This is because the enthalpy difference between

*yansun.yao@usask.ca
†xieyu@jlu.edu.cn

compounds and their elemental components increases under compression due to the increment of both PV work and internal energy U. Further analysis suggests that a low bulk modulus, a large atomic volume of La, and weakened interatomic interactions at high pressure are responsible for the decomposition of M_xLa_y. The predicted decomposition of these compounds at high pressures suggests that the usage of lanthanum intermetallic compounds should be carefully considered in the applications that are strongly related to extreme conditions, such as the aerospace industry.

II. COMPUTATIONAL METHODS AND DETAILS

Our search simulations for structures of the lanthanum intermetallic compounds were performed by using the swarm-intelligence-based CALYPSO structure prediction method and its same-name code, which can be used to predict stable structures depending on the given chemical composition by combining with *ab initio* total-energy calculations [38–40]. Structural searches for Mg_xLa_y and Al_xLa_y at 0, 20, 50, and 100 GPa used simulation cells consisting of 1, 2, and 4 formula units (f.u.). For other systems, the searches were performed at 0, 100, 200, and 300 GPa, using simulation cells consisting of 2 f.u. In addition, the searches for Ga_2La, Pb_3La, Pb_4La_5, Bi_3La, and $BiLa_2$ were also performed at 400 GPa since they have not decomposed at 300 GPa. Besides, variable-composition structure searches were performed for Mg_xLa_y and Al_xLa_y to look for new stoichiometries, which yielded thousands of structures of Mg_xLa_y at 100, 200, and 300 GPa and of Al_xLa_y at 200 and 300 GPa, respectively.

The Vienna Ab initio Simulation Package (VASP) within the framework of density functional theory (DFT) was used for structural relaxations and electronic property calculations [41,42]. The Perdew-Burke-Ernzerhof (PBE) functional in the generalized gradient approximation (GGA) was used to describe the exchange-correlation potential [43]. The electron-ion interactions were represented by means of the all-electron projector augmented wave (PAW) method [44], where $5s^25p^66s^25d^1$ are treated as the valence states of La. The plane-wave energy cutoff of 500 eV and a dense k-point grid of spacing $2\pi \times 0.03$ Å^{-1} in the Monkhorst-Pack scheme were used to sample the Brillouin zone and ensure the enthalpy calculations converged with an error of less than 1 meV/atom [45]. Structural relaxations were performed with forces converged to less than 0.001 eV Å^{-1}. To examine the dynamic stabilities of predicted phases, phonon calculations were performed by using a supercell approach with the finite displacement method which is implemented in the PHONOPY code [46]. Bader's quantum theory of atoms in molecules (QTAIM) analysis was employed for the charge transfer calculation [47]. The bonding was further analyzed by calculating the projected crystal orbital Hamilton populations (pCOHPs) [48] and the negative of the pCOHP integrated to the Fermi level (−IpCOHP) using the LOBSTER package [49,50]. To check the magnetic properties of La compounds, we have performed spin-polarization calculations for all compounds in the low-pressure regime (50 GPa). Our trial set of magnetic configurations involves 1 ferromagnetic (FM) and 4 antiferromagnetic (AFM) configurations for the Fd-3m structure of Al_2La and Ga_2La, and 11 AFM configurations for $P6/mmm$ of Ga_2La (as shown in Fig. S23 of the Supplemental Material [51]). These AFM configurations are exhaustive up to a supercell with four La atoms and were generated using the derivative structure enumeration library ENUMLIB [52]. For other compounds, we considered two AFM configurations for every structure (Fig. S24 of the Supplemental Material [51]). The enthalpy of formation per atom of M_xLa_y (M = metals) was calculated by using the following formula: $\Delta H(M_xLa_y)=[H(M_xLa_y)-xH(M)-yH(\mathrm{La})]/(x+y)$, where H represents the enthalpy per formula unit for each compound.

III. RESULTS AND DISCUSSION

We first explored the high-pressure structures of M_xLa_y over experimentally known stoichiometries at various pressures [53–58]. The thermodynamic stabilities of M_xLa_y were evaluated by calculating their formation enthalpies with respect to the dissociation into individual elemental components between 0 and 300 GPa (Fig. 1). We have considered possible magnetic configurations (Figs. S23 and S24 of the Supplemental Material [51]) for all structures below 50 GPa by performing spin-polarized calculations, where all the phases are nonmagnetic. Thus, we use spin-unpolarized results for the following discussions. At 0 GPa, all known structures of M_xLa_y have been successfully reproduced, which establishes the accuracy of the employed structure search method. Under compression, most of these compounds undergo phase transitions to high-pressure structures. Strikingly, all M_xLa_y compounds are found to eventually decompose into the elemental solids at sufficient compression. Detailed information about the structures and decomposition pressures of all compounds is shown in Fig. 1 and in Table S1 of the Supplemental Material [51]. For the compounds between La and group IIA elements (Be, Mg), the decomposition pressures are quite low. $Be_{13}La$, the only known Be_xLa_y compound, decomposes at 46 GPa without undergoing any phase transitions. All Mg_xLa_y compounds decompose at pressures below 35 GPa. In particular, MgLa and Mg_2La transform into $P4/nmm$ and $I4_1/amd$ structures at about 6 and 16 GPa before decomposing at 21 and 19 GPa, respectively. For the compounds between La and group IIIA elements (Al, Ga, In, and Tl), the decomposition pressures are relatively high. In this group, Al_xLa_y and Ga_xLa_y have the lowest and highest decomposition pressures, respectively. Al_2La, the most stable phase in Al_xLa_y, decomposes at 80 GPa without any phase transitions. AlLa, Al_3La, and $Al_{11}La_3$ undergo phase transitions to $P4_2/mmc$, $P2_1/m$, and Fm-3m structures at 33, 16, and 45 GPa, and decompose at 48, 80, and 53 GPa, respectively. Like Al_2La, Ga_2La is the most stable phase in Ga_xLa_y, but it differs from the former since it undergoes one phase transition to the Fd-3m phase at 18 GPa, before it decomposes near 350 GPa. Ga_3La_5 and GaLa undergo phase transitions to $Cmmm$ and $Pmma$ structures at 22 and 5 GPa, and decompose at 136 and 163 GPa, respectively. Ga_6La undergoes two consecutive transformations to $Cmcm$ at 40 GPa and to C_2 at 150 GPa, and then decomposes at 225 GPa. In_xLa_y and Tl_xLa_y behave similarly by having the same ambient structures and most of the high-pressure structures, but In_xLa_y undergo phase transitions and decomposition at higher pressures. Specifically, $InLa_3$ and

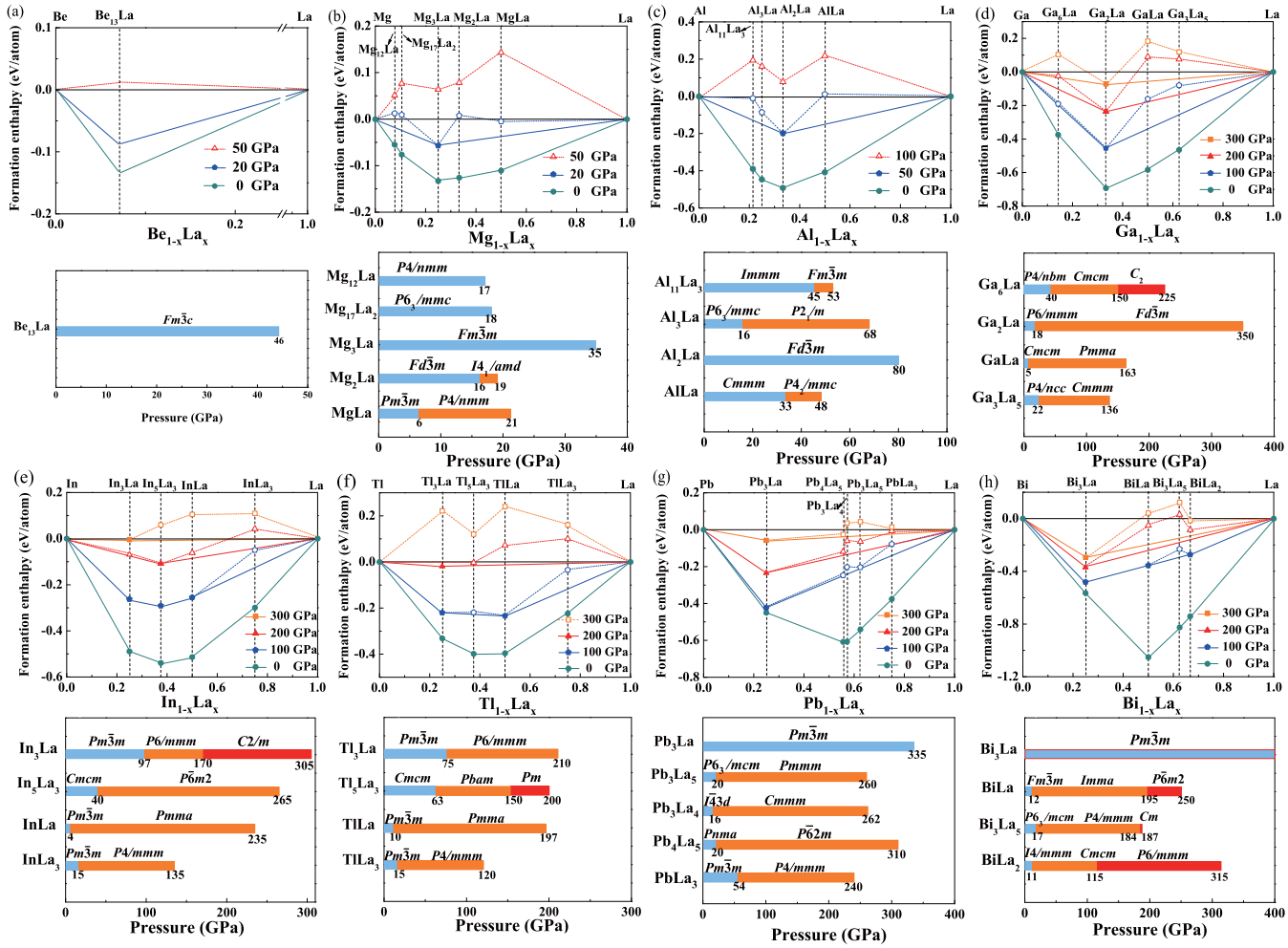

FIG. 1. Thermodynamic stabilities with respect to M and La, and phase diagrams of various compounds (a) Be_xLa_y, (b) Mg_xLa_y, (c) Al_xLa_y, (d) Ga_xLa_y, (e) In_xLa_y, (f) Tl_xLa_y, (g) Pb_xLa_y, and (h) Bi_xLa_y at 0 K and different pressures. The stoichiometries of structures lying on the convex hull (solid line) are stable against decomposition at a given pressure, while those located above the convex hull (dashed line) are either unstable or metastable. The stoichiometries studied here are experimentally known at ambient pressure.

$TlLa_3$ transform into the same $P4/mmm$ structure before they decompose at 135 and 120 GPa, respectively, while InLa and TlLa transform into *Pmma* structure and decompose at 235 and 197 GPa, respectively. For In_3La and Tl_3La, they undergo the same phase transition to $P6/mmm$ as pressure increases, but In_3La has one additional transition to a $C2/m$ structure before decomposition. In_3La and Tl_3La decompose at 305 and 210 GPa, respectively. In_5La_3 and Tl_5La_3 are the only pair in this group that have different transition sequences. In_5La_3 transforms to P-6m2 at 40 GPa, while Tl_5La_3 transforms to *Pbam* at 63 GPa and to *Pm* at 150 GPa. They decompose at 265 and 200 GPa, respectively.

For Pb_xLa_y and Bi_xLa_y compounds, the decomposition pressures are the highest. Pb_3La maintains the Pm-3m structure until it decomposes at 335 GPa. $PbLa_3$, Pb_4La_5, Pb_3La_4, and Pb_3La_5 undergo phase transitions into $P4/nmm$, P-6m2, *Cmmm*, and Pm-3m structures at 54, 20, 16, and 20 GPa, then decompose at 240, 310, 262, and 260 GPa, respectively. Strikingly, the decomposition pressures of Bi_xLa_y are extremely higher. At 400 GPa, the most stable phase in the group, Bi_3La, is still stable. From the enthalpy calculation, we estimate the decomposition pressure of Bi_3La to be over 700 GPa, assuming it does not undergo additional phase transitions before decomposition. Besides, $BiLa_2$, Bi_3La_5, and BiLa all undergo two consecutive phase transitions as the pressure increases. They transform to *Cmcm*, $P4/mmm$, and *Imma* at at 11, 17, and 12 GPa, then to $P6/mmm$, *Cm*, and P-6m2 at 115, 184, and 195 GPa and decompose at 315, 187, and 250 GPa, respectively. Since Pb, Bi, and La are all heavy elements, the relativistic effect might be strong enough to alter the thermodynamic stability of the compounds. Thus, we reconstructed the convex hulls and phase diagrams of Pb_xLa_y and Bi_xLa_y by including the spin-orbit-coupling (SOC) effects as shown in Fig. S25 of the Supplemental Material [51]. Although some of the phase transition and decomposition pressures are postponed by considering SOC, the shape of the convex hulls and phase diagrams and the trend of the decomposition remain the same, suggesting that SOC only plays a minor role in determining the phase stability of these heavy intermetallic compounds.

We note that the stoichiometries are based on the experimental knowledge of M_xLa_y at ambient conditions. However,

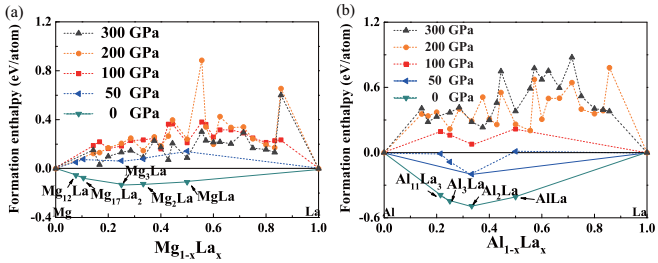

FIG. 2. The convex hulls of different stoichiometries of (a) Mg_xLa_y and (b) Al_xLa_y compounds at 0, 50, 100, 200, and 300 GPa. All of the studied phases are unstable at pressures above 100 GPa.

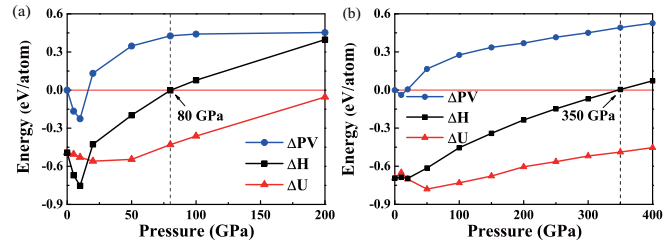

FIG. 3. ΔH, ΔU, and $P\Delta V$ versus pressure for (a) Al_2La, Al + La mixture, and (b) Ga_2La, Ga + La mixture, where Al (Ga) + La is chosen as the reference. Here, the dashed lines represent the decomposition pressure. Al_2La decomposes at around 80 GPa, while Ga_2La decomposes at around 350 GPa.

it is well known that high pressure can alter the electronic structure of elements and lead to the formation of new stoichiometries [33,37,59], which may postpone the decomposition or further stabilize the system. To this end, we have performed variable-composition structure searches, which are computationally very demanding, of Mg_xLa_y at 100, 200, and 300 GPa, and Al_xLa_y at 200 and 300 GPa as representative since they have low decomposition pressures among the studied compounds. The results show that all stoichiometries we searched are still unstable at 100, 200, and 300 GPa (Fig. 2). But, the formation enthalpies of four Al_xLa_y and almost all Mg_xLa_y stoichiometries become lower at 300 GPa, indicating that they may become stable again at higher pressures. Specifically, Mg_3La is the most stable phase below 100 GPa, while at 200 and 300 GPa, Mg_2La and Mg_5La are the most stable ones, respectively. The Al_4La_5 and Al_5La_3 have the lowest formation enthalpy at 200 and 300 GPa, respectively. The high-pressure behaviors of other (yet more stable) M_xLa_y compounds are expected to follow the same trend, but with significantly higher pressures to reenter the phase diagram.

To elucidate the mechanism of the pressure-induced decomposition in M_xLa_y, we examined the evolution of the enthalpy difference between the compounds and their elemental mixtures as a function of pressure. The enthalpy difference at 0 K is calculated as $\Delta H = \Delta U + P\Delta V$, where ΔU and $P\Delta V$ are the difference in internal energy and that in the PV work, respectively. Here P is the external pressure, the same for both the compound and elemental mixture. When a compound has a larger volume than its elemental components, $P\Delta V$ is positive. Since Al_2La and Ga_2La have similar structures and both are the most stable phase in their respective groups, they are analyzed as representative species. The pressure dependence of ΔH, ΔU, and $P\Delta V$ for Al_2La and Ga_2La are presented in Fig. 3. (For other compounds, the results are depicted in Figs. S7 to S14 of the Supplemental Material [51].) At low pressures above zero, $P\Delta V$ is negative for both Al_2La and Ga_2La. With increasing pressure, $P\Delta V$ increases rapidly and becomes positive at 16 and 20 GPa, respectively. This result indicates that the PV work for the compound becomes larger than that of the elemental mixture at high pressure, which is uncommon. $P\Delta V$ of Al_2La and Ga_2La increases by 0.43 and 0.50 eV as the pressure increases to 80 and 350 GPa, respectively. At the same pressures, ΔU of Al_2La and Ga_2La increases by 0.06 and 0.19 eV, respectively. It is therefore established that both $P\Delta V$ and ΔU contribute to the increment of ΔH in the compounds which results in their decomposition at sufficient compression. In return, the decomposition pressures of the compounds are also determined by these two factors. The decomposition pressure of Ga_2La is 350 GPa, which is much higher than the 80 GPa of Al_2La. At zero pressure, ΔH of Al_2La is -0.49 eV, higher than the -0.69 eV of Ga_2La. If the increase rates of ΔH were identical in Al_2La and Ga_2La, the decomposition pressure of Ga_2La should be 1.4 times larger than Al_2La. But, the actual increase rate of ΔH in Ga_2La is much lower than that in Al_2La, which results in an even larger decomposition pressure for Ga_2La. Also, the increase rate of $P\Delta V$ of Ga_2La is smaller than that of Al_2La at higher pressures. The increment of $P\Delta V$ of Ga_2La is about 0.06 eV when the pressure increases to 50 GPa, while it is 0.25 eV for Al_2La. Besides, the increase of ΔU for Ga_2La is also smaller than that of Al_2La. ΔU of Ga_2La is about 0.05 eV when the pressure increases 50 GPa, which is much lower than the 0.1 eV of Al_2La. Therefore, Ga_2La is more difficult to decompose than Al_2La.

To probe the physical origin of the pressure-induced decomposition, we examined the evolution of the compound volumes as a function of pressure. The calculated volume of Al_2La and Ga_2La, and those of their elemental components, and the differences are shown in Figs. 4(a) and 4(b). It can be seen that at ambient pressures, the volumes of Al_2La and Ga_2La are smaller than the volumes of elements. Thus, ΔV is negative, which is thermodynamically allowed and the case for most compounds. Upon compression, ΔV increases rapidly in the low-pressure regime (50 GPa). ΔV becomes positive at around 5 and 20 GPa for Al_2La and Ga_2La, respectively, suggesting that the elements are more compressible than the compounds. As a consequence, $P\Delta V$ becomes positive and increases with the pressure. The change of material volume under pressure is determined by the compressibility as reflected in the bulk modulus and ambient volume. Elemental La has a low bulk modulus of 28 GPa and a large volume of 37 Å^3 per atom. Thus, a small compression can induce a large volume change for La. The calculated volume differences in volumes at zero and finite pressures are shown in Figs. 4(c) and 4(d). It is clear that the volume of La rapidly decreases below 50 GPa, which causes the increment of ΔV. Interestingly, ΔV tends to decrease when pressure is higher than 50 GPa [Figs. 4(a) and 4(b)]. Noteworthy is that $P\Delta V$ keeps increasing in a wide pressure range since the

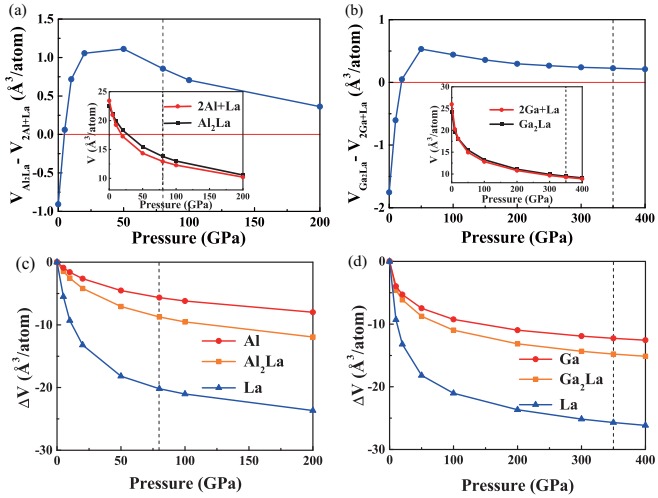

FIG. 4. (a), (b) The volume differences between the compound (Al_2La, Ga_2La) and La + M (M= Al, Ga) are shown in figure a, b, respectively. As earlier, the dashed line represents the decomposition pressure. (c), (d) The ΔV ($\Delta V = V_{pressure} - V_0$) of Al_2La and Ga_2La versus pressure are shown in figure c, d, respectively. V_0 represents the volume at 0 GPa.

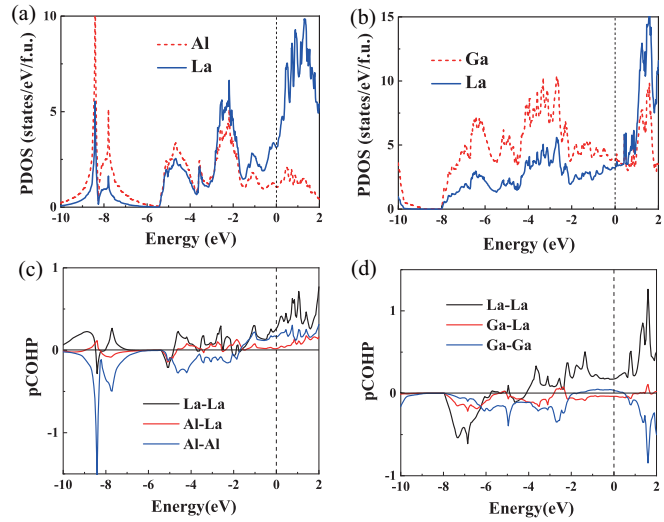

FIG. 6. Calculated (a), (b) PDOS and (c), (d) pCOHP for (a), (c) Al_2La at 80 GPa and (b), (d) Ga_2La at 350 GPa. The states are aligned at the Fermi level (vertical dashed lines).

decreasing rate of the ΔV is smaller than the increasing rate of the pressure, resulting in a slow increment of the $P\Delta V$ term. Overall, our analysis suggests that the increased $P\Delta V$ term is due to the drastically changed ΔV at low pressures, and the increase of ΔV is mainly caused by the sharply decreased volume of La at low pressures.

We then proceeded to understand the interatomic interactions in the compounds. As a measure of interatomic interactions, the charge transfer between atoms in the compounds is calculated using Bader charge analysis. The results for Al_2La and Ga_2La are shown in Fig. 5 (results for other compounds are in Figs. S15–S20 in the Supplemental Material [51]). At ambient pressure, about one electron is transferred from each La atom to neighboring Al atoms in Al_2La, while 1.3 electrons are transferred in Ga_2La. This is consistent with a stronger electrostatic interaction in Ga_2La than in Al_2La, which is mainly caused by the difference of electronegativity between the elements. Since the electronegativity difference between Al and La (0.5) is smaller than that of Ga and La (0.7), fewer electrons are transferred from La to Al than from La to Ga. However, the charge transfer is suppressed under compression (Fig. 5), indicating a smaller electrostatic interaction binding the compounds. At the decomposition pressures, the charge transfer becomes almost zero. Due to the reduction in electrostatic interaction, the internal energy of the compounds increases quicker than the elements, which results in an increment of ΔU. Moreover, the reduced charge transfer at high pressures suggests that the electronegativity difference between La and M becomes smaller, resulting from the changing electronegativity of both elements at high pressure.

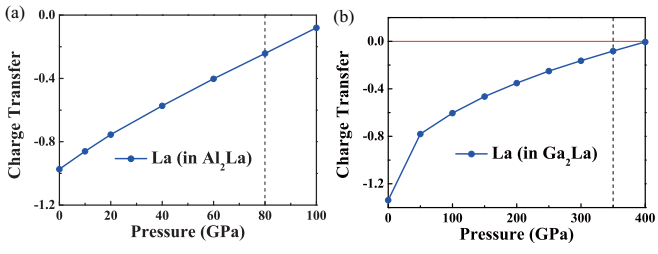

FIG. 5. The Bader charge of La in (a) Al_2La from 0 to 100 GPa and (b) Ga_2La from 0 to 400 GPa. The charge transfer decreases almost linearly with increasing pressures, which means that the interaction between Al (Ga) and La gradually decreases at high pressures.

Recently, the electronegativity of most elements at high pressure was calculated by Rahm *et al.* [60] and Dong *et al.* [61]. Both works suggested the electronegativity of the elements will decrease under compression. In particular, the electronegativity of La should decrease much faster than the main group metals [60]. Thus, the electronegativity difference between La and *M* should increase at high pressures, which seems to contradict our observation in La compounds. To understand this discrepancy, we analyze the electron distributions in Al_2La and Ga_2La by calculating the electron localization function (ELF) as shown in Fig. S22 of the Supplemental Material [51]. The ELF shows a great tendency of electron localization between *M* and *M*, suggesting the interactions between *M* and *M* might also be very important. We then use the crystal orbit Hamiltonian population (COHP), which counts the population of wave functions on two atomic orbitals of a pair of selected atoms, and projected density of states (PDOS) to explore the bonding properties in these compounds. Although the calculated PDOS shows a large overlap between *M* and La over a wide energy range, the calculated COHP reveals there is no covalent bonding between them (Fig. 6), so the interaction between the two should be mainly ionic. On the other hand, the COHP shows that the bonding of *M*-*M* and La-La is ionic or metallic. The integrated COHP (ICOHP) up to the Fermi level is shown in Table S2 of the Supplemental Material [51]. The ICOHP of

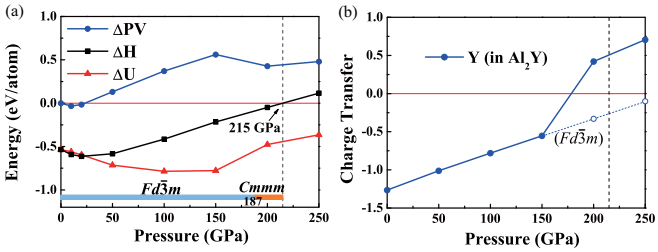

FIG. 7. (a) The ΔH, ΔU, $P\Delta V$ versus pressure for Al_2Y and Al + Y mixtures, where Al + Y is chosen as the reference. (b) The Bader charge of Al_2Y from 0 to 250 GPa. As earlier, the dashed line represents the decomposition pressure. Al_2Y decomposes at about 215 GPa.

M-*M* and La-La pairs is always larger than that of the *M*-La pair, suggesting the *M*-*M* and La-La interactions might be stronger than the *M*-La interaction. Therefore, the electron distribution of La intermetallic compounds not only relies on the interaction between *M* and La but is also affected by the *M*-*M* and La-La interactions. Thus, the charge transfer at high pressure cannot be simply explained by the change of the atomic electronegativity of elements but is a coupled effect of many different interactions.

Our analysis suggests there are several determining factors for the decomposition of M_xLa_y at high pressure: a low bulk modulus, a large volume of La, and weakened interaction between La and M at high pressure. It is reasonable to suggest that a similar decomposition phenomenon may occur in other La-like intermetallic compounds. For example, Y has a low bulk modulus of 41 GPa and a large volume of 33 Å^3 per atom, and an electronegativity similar to that of La. Thus, we carried out the same analysis for Al_2Y, which is the most stable phase in the Al-Y system at ambient pressure [62]. We found that Al_2Y transforms from Fd-3*m* into *Cmmm* structure at around 187 GPa, then decomposes at 215 GPa. From 0 to 215 GPa, the increase of $P\Delta V$ and ΔU is 0.44 and 0.11 eV, respectively, which confirms that $P\Delta V$ and ΔU contribute to the decomposition, and the change of $P\Delta V$ is larger than ΔU. Remarkably, we found that the charge transfer from Y to Al also gradually decreases as pressure increases [Fig. 7(b)]. At 180 GPa, the charge transfer is reduced to zero, and after that the electrons begin to transfer from Al to Y. At decomposition pressure (215 GPa), around 0.5 electron is transferred from Al to Y. This suggests that the decrease of electronegativity difference between Al and Y is larger than that between Al and La at high pressures. Besides, the charge transfer in Fd-3*m* structure is also shown in Fig. 7(b). The decrease of the charge transfer from Y to Al in Fd-3*m* structure is smaller than that in *Cmmm* structure. This suggests that the high-pressure phase transition can also affect the charge transfer and the decrease of electronegativity in the compound. The unusual phenomenon is intriguing, which will certainly invite more studies on La-like intermetallic compounds in the future.

IV. CONCLUSION

In summary, we have explored the uncharted stoichiometries and structures of lanthanum intermetallic compounds at high pressures using the swarm-intelligence-based CALYPSO method. We found a common yet intriguing phenomenon for this group of compounds, which is that all compounds will decompose to elemental solids at sufficient compression. We elucidated the mechanism underlying the decomposition by analyzing the changes of the *PV* work and the internal energy in both the compounds and their elemental components under increasing pressure. The results suggest that the enhanced $P\Delta V$ term and ΔU between the compound and its elemental mixture contribute to the decomposition, which is caused by a low bulk modulus of La and reduced interatomic interactions in the compound at high pressures. Further analysis of charge transfer shows that the increment of internal energy in lanthanum intermetallic compounds is strongly affected by the relative changes of electronegativity in elements and the interactions between elements at high pressure. Moreover, our results have important implications for other binary intermetallic compounds such as Al_2Y which shares the same decomposition mechanism. The pressure-induced decomposition of intermetallic compounds is against our intuition that external pressure always makes materials more stable and dense, which provides an important point of consideration for future material synthesis using the pressure parameter.

ACKNOWLEDGMENTS

This work is supported by the Fundamental Research Funds for the Central Universities (Jilin University, JLU), the Natural Sciences and Engineering Research Council of Canada (NSERC), the National Natural Science Foundation of China (Grants No. 11534003, No. 11874176, and No. 11974135), Science Challenge Project No. TZ2016001, the Program for JLU Science and Technology Innovative Research Team (JLUSTIRT), and National Key Research and Development Program of China (under Grant No. 2016YFB0201201). We used the computing facilities at the High-Performance Computing Centre of Jilin University.

[1] G. Fleming, S. Liu, and T. Loucks, Phys. Rev. Lett. **21**, 1524 (1968).
[2] B. Sundqvist, Phys. Rev. Lett. **69**, 2693 (1992).
[3] X. W. Wang, B. N. Harmon, Y. Chen, K. M. Ho, C. Stassis, and W. Weber, Phys. Rev. B **33**, 3851 (1986).
[4] S. Bağci, H. M. Tütüncü, S. Duman, and G. P. Srivastava, Phys. Rev. B **81**, 144507 (2010).
[5] A. Pol, T. R. Barends, A. Dietl, A. F. Khadem, J. Eygensteyn, M. S. Jetten, and H. J. Op den Camp, Environ. Microbiol. **16**, 255 (2014).
[6] K. Binnemans, P. T. Jones, B. Blanpain, T. Van Gerven, Y. Yang, A. Walton, and M. Buchert, J. Clean Prod. **51**, 1 (2013).
[7] L. W. Nixon, D. A. Papaconstantopoulos, and M. J. Mehl, Phys. Rev. B **78**, 214510 (2008).

[8] M. Debessai, J. J. Hamlin, and J. S. Schilling, Phys. Rev. B **78**, 064519 (2008).

[9] D. A. Dikin, M. Mehta, C. W. Bark, C. M. Folkman, C. B. Eom, and V. Chandrasekhar, Phys. Rev. Lett. **107**, 056802 (2011).

[10] L. Li, C. Richter, J. Mannhart, and R. C. Ashoori, Nat. Phys. **7**, 762 (2011).

[11] P. Delugas, A. Filippetti, V. Fiorentini, D. I. Bilc, D. Fontaine, and P. Ghosez, Phys. Rev. Lett. **106**, 166807 (2011).

[12] K. Michaeli, A. C. Potter, and P. A. Lee, Phys. Rev. Lett. **108**, 117003 (2012).

[13] M. J. Han, H. Kino, and T. Kotani, Phys. Rev. B **90**, 035127 (2014).

[14] R. Scherwitzl, S. Gariglio, M. Gabay, P. Zubko, M. Gibert, and J. M. Triscone, Phys. Rev. Lett. **106**, 246403 (2011).

[15] V. Srivastava, S. P. Sanyal, and M. Rajagopalan, Physica B: Condens. Matter **403**, 3615 (2008).

[16] Y. Ö Çiftci, K. Çolakoğlu, E. Deligöz, and Ü. Bayhan, J. Mater. Sci. Technol. **28**, 155 (2012).

[17] R. Lou, B.-B. Fu, Q. N. Xu, P.-J. Guo, L.-Y. Kong, L.-K. Zeng, J.-Z. Ma, P. Richard, C. Fang, Y.-B. Huang *et al.*, Phys. Rev. B **95**, 115140 (2017).

[18] J. Nayak *et al.*, Nat. Commun. **8**, 13942 (2017).

[19] F. F. Tafti *et al.*, Phys. Rev. B **95**, 014507 (2017).

[20] R. Singha, B. Satpati, and P. Mandal, Sci. Rep. **7**, 6321 (2017).

[21] M. Escudero-Escribano *et al.*, Science **352**, 73 (2016).

[22] D. Pukazhselvan, V. Kumar, and S. K. Singh, Nano Energy **1**, 566 (2012).

[23] L. Zhang, Y. Wang, J. Lv, and Y. Ma, Nat. Rev. Mater. **2**, 17005 (2017).

[24] Y. Ma, M. Eremets, A. R. Oganov, Y. Xie, I. Trojan, S. Medvedev, A. O. Lyakhov, M. Valle, and V. Prakapenka, Nature (London) **458**, 182 (2009).

[25] Y. Ma, A. R. Oganov, and Y. Xie, Phys. Rev. B **78**, 014102 (2008).

[26] J. Lv, Y. Wang, L. Zhu, and Y. Ma, Phys. Rev. Lett. **106**, 015503 (2011).

[27] H. Wang, J. S. Tse, K. Tanaka, T. Iitaka, and Y. Ma, Proc. Natl. Acad. Sci. USA **109**, 6463 (2012).

[28] Y. Yao, J. S. Tse, K. Tanaka, F. Marsiglio, and Y. Ma, Phys. Rev. B **79**, 054524 (2009).

[29] Y. Yao, J. S. Tse, and K. Tanaka, Phys. Rev. B **77**, 052103 (2008).

[30] Y. Yao, D. D. Klug, J. Sun, and R. Martonak, Phys. Rev. Lett. **103**, 055503 (2009).

[31] H. Fukuoka, K. Suekuni, T. Onimaru, and K. Inumaru, Inorg. Chem. **50**, 3901 (2011).

[32] H. Fukuoka and S. Yamanaka, Phys. Rev. B **67**, 094501 (2003).

[33] H. Liu, I. I. Naumov, R. Hoffmann, N. W. Ashcroft, and R. J. Hemley, Proc. Natl. Acad. Sci. USA **114**, 6990 (2017).

[34] Z. M. Geballe, H. Liu, A. K. Mishra, M. Ahart, M. Somayazulu, Y. Meng, M. Baldini, and R. J. Hemley, Angew. Chem. Int. Ed. Engl. **57**, 688 (2018).

[35] A. P. Drozdov *et al.*, Nature (London) **569**, 528 (2019).

[36] M. Somayazulu, M. Ahart, A. K. Mishra, Z. M. Geballe, M. Baldini, Y. Meng, V. V. Struzhkin, and R. J. Hemley, Phys. Rev. Lett. **122**, 027001 (2019).

[37] F. Peng, Y. Sun, C. J. Pickard, R. J. Needs, Q. Wu, and Y. Ma, Phys. Rev. Lett. **119**, 107001 (2017).

[38] Y. Wang, J. Lv, L. Zhu, and Y. Ma, Phys. Rev. B **82**, 094116 (2010).

[39] Y. Wang, J. Lv, L. Zhu, and Y. Ma, Comput. Phys. Commun. **183**, 2063 (2012).

[40] B. Gao, P. Gao, S. Lu, J. Lv, Y. Wang, and Y. Ma, Sci. Bull. **64**, 301 (2019)

[41] Y. Wang and J. P. Perdew, Phys. Rev. B **43**, 8911 (1991).

[42] Kresse and Furthmuller, Phys. Rev. B **54**, 11169 (1996).

[43] J. P. Perdew and Y. Wang, Phys. Rev. B **45**, 13244 (1992).

[44] P. E. Blochl, Phys. Rev. B **50**, 17953 (1994).

[45] H. J. Monkhorst and J. D. Pack, Phys. Rev. B **13**, 5188 (1976).

[46] A. Togo, F. Oba, and I. Tanaka, Phys. Rev. B **78**, 134106 (2008).

[47] W. Tang, E. Sanville, and G. Henkelman, J. Phys.: Condens. Matter **21**, 084204 (2009).

[48] R. Dronskowski and P. E. Bloechl, J. Phys. Chem. **97**, 8617 (1993).

[49] V. L. Deringer, A. L. Tchougréeff, and R. Dronskowski, J. Phys. Chem. A **115**, 5461 (2011).

[50] S. Maintz, V. L. Deringer, A. L. Tchougréeff, and R. Dronskowski, J. Comput. Chem. **37**, 1030 (2016).

[51] See Supplemental Material at http://link.aps.org/supplemental/10.1103/PhysRevB.101.184113 for structure information, the calculated difference of enthalpy, energy and *PV* work, the Bader analysis, phonon density of states, the ELF and the IpCOHP, magnetic configurations, and the SOC calculation, which includes Refs. [38–43,49,50,52].

[52] G. L. W. Hart, L. J. Nelson, and R. W. Forcade, Comput. Mater. Sci. **59**, 101 (2012)

[53] W. B. Holzapfel, Acta Cryst. B **70**, 429 (2014)

[54] A. Berche, F. Marinelli, J. Rogez, and M. C. Record, Thermochim. Acta **499**, 65 (2010)

[55] J. A. Abraham, G. Pagare, S. S. Chouhan, and S. P. Sanyal, Comput. Mater. Sci. **81**, 423 (2014)

[56] H. M. Tutuncu, E. Karaca, H. Y. Uzunok, and G. P. Srivastava, Phys. Rev. B **97**, 174512 (2018)

[57] G. Borzone, A. M. Cardinale, N. Parodi, and G. Cacciamani, J. Alloy Compd. **247**, 141 (1997)

[58] S. P. Yatsenko, A. A. Semyannikov, B. G. Semenov, and K. A. Chuntonov, J. Less-Common Met. **64**, 185 (1979)

[59] Y. Xie, A. R. Oganov, and Y. Ma, Phys. Rev. Lett. **104**, 177005 (2010).

[60] M. Rahm, R. Cammi, N. W. Ashcroft, and R. Hoffmann, J. Am. Chem. Soc. **141**, 10253 (2019).

[61] X. Dong, A. R. Oganov, G. Qian, X.-F. Zhou, Q. Zhu, and H.-T. Wang, arXiv:1503.00230.

[62] X. Niu, Z. Huang, H. Wang, L. Hu, and B. Wang, Rare Met. Mater. Eng. **47**, 1325 (2018).